Int. J. Electrochem. Sci., 12 **(2017)** 5704 – 5722, doi: 10.20964/2017.06.90

International Journal of
ELECTROCHEMICAL
SCIENCE
www.electrochemsci.org

Electrochemical Corrosion Behavior of TC11 Alloy in Sulfate Solution at High Temperature and High Pressure

Lei Zha[1, 2], *Heping Li*[1,*], *Ning Wang*[1], *Sen Lin*[1] *and Liping Xu*[1]

[1] Key Laboratory of High-temperature and High-pressure Study of the Earth's Interior, Institute of Geochemistry, Chinese Academy of Sciences, Guiyang 550081, P. R. China
[2] University of Chinese Academy of Sciences, Beijing 100049, P. R. China
[*]E-mail: liheping@vip.gyig.ac.cn

Received: 14 March 2017 / *Accepted:* 30 April 2017 / *Published:* 12 May 2017

TC11 alloy is a potential alloy for use in high temperature aggressive water environments. The electrochemistry and corrosion behavior of TC11 alloy is investigated in sodium sulfate solution at high temperature and high pressure using various in situ electrochemical techniques, i.e., open circuit potential (OCP), potentiodynamic polarization (PDP), and electrochemical impedance spectroscopy (EIS) measurements. The effect of sodium sulfate concentration, temperature, and pressure on the electrochemical corrosion behavior of the alloy has been explored. The results indicate that the increase of either concentration or temperature and pressure shift the value of the corrosion potential (E_{corr}) for the alloy toward the negative direction, while increasing the values of corrosion current density (i_{corr}) and corrosion rate (R_{corr}). The values of oxide film resistance (R_f) and charge transfer resistance (R_{ct}) confirm these results. The EIS and polarization results are in good agreement with each other.

Keywords: Titanium alloy; EIS; Corrosion; High temperature; High pressure

1. INTRODUCTION

Titanium alloys belong to a category of comparatively new engineering materials primarily utilized in many applications in the marine, chemical industries and aerospace due to their strong mechanical properties and excellent corrosion resistance. The prominent corrosion resistance of titanium alloys in a lot of industrial conditions results from a protective passive film that is formed on the alloy surface [1]. TC11 alloy is a kind of high temperature resistant, high Al-equivalent, high-strength (α+β) dual-phase corrosion resistance titanium alloy, the nominal composition of which, Ti-6.5Al-3.5Mo-1.5Zr-0.3Si, can provide long-term work under 500 °C. TC11 alloy is widely used in

manufacturing complex parts of aeroengines, and more recently used in the industrial field. They are the materials chosen employ in autoclave liners and interior components such as nozzles, valves, agitator blades, during the high pressure acid leaching (HPAL) of ores [2]. Titanium alloys are recommended for harsh environments of supercritical water oxidation (SCWO) [3] and are promising materials for manufacturing tube supports in steam generator (SG) systems in nuclear reactor systems.

During service they are subjected to extreme conditions of acidity, high salt (sulfate, chloride), high temperature, and high pressure. Even though extremely erosion-resistant and corrosion resistance, titanium alloys also have the possibility of local corrosion and general corrosion, and their corrosion resistance may be greatly reduce in a severe corrosion environment. Corrosion damage is expensive to repair and may cause unwanted process downtime [2]. Thus, it is necessary to study the problems concerning the safety of titanium alloy applications in high pressure hydrothermal environments.

However, there are only a few researches on electrochemical corrosion behavior of metals in high pressure hydrothermal environments [4–8]. Many papers have been published regarding titanium corrosion and electrochemistry at ambient temperature. Studies of titanium-based alloys at high temperature are still relatively scarce. Although the effect of temperature [9–12], and sulfate concentration [11–13] on the corrosion has been studied, these studies specifically focus on the corrosion behavior in low pH conditions. Additionally, the influence of pressure [14–16] on the corrosion of metals has been reported. To the author's knowledge, there is no literature related to in situ electrochemical corrosion of titanium alloys over the range of temperatures and pressures considered in this study.

The present study therefore takes on great significance as it examines and evaluates the effect of Na_2SO_4 concentration, temperature, and pressure on the corrosion and passivating characters of TC11 alloy at 200 to 350 (±1) °C under a pressure of 10 to 30 (±0.5) MPa. These temperatures and pressures are often experienced in many industrial processes such as power plant systems, SCWO systems, wet air oxidation systems, HPAL processes, and geothermal systems. During the research, we examined the corrosion rate as well as corrosion mechanism by in situ electrochemical techniques. This study aims to acquire quantitative data about promising materials for commercial high temperature water systems. As a consequence, the research of electrochemical corrosion is meaningful in the practical application as well as theoretical standpoint.

2. EXPERIMENTAL

2.1. Electrochemical methods

All the electrochemical tests were performed utilizing a Princeton Applied Research (PAR) 2263 electrochemical workstation. The OCP tests were carried out till to reach a stable value with a change of less than 2 mV min^{-1}. The PDP experiments on TC11 alloy were performed from −250 mV vs OCP up to 1600 mV vs Ag/AgCl with a scan rate of 1 mV s^{-1}. The EIS measurements on TC11 alloy were conducted with a peak-to-peak amplitude of 10 mV at OCP in the frequency range of 10^{-2}–10^{4} (10^{5}) Hz. ZSimpWin 3.10 (2002) was utilized to fit the EIS data.

2.2. Apparatus configuration

The electrochemical tests were performed using a home-made multifunctional autoclave. The autoclave was machined using stainless steel with a titanium alloy liner. Passivation treatment was performed before the experiments to ensure the chemical inertness of the titanium alloy liner of the autoclave at elevated temperatures. The heating of the whole autoclave is provided by a resistance heated furnace and controlled by a temperature regulator/programmer (±1 °C) connected with k-type thermocouples. A pressure sensor was used to record the pressure in the autoclave. The working electrode was a titanium alloy cone frustum, made from a TC11 bar. The auxiliary electrode was a platinum electrode. Both the working and counter electrodes were leaving a working area of 0.43 cm^2. An Ag/AgCl electrode filled with saturated KCl solution was used as the reference electrode. The reference electrode was kept at room temperature and connected to autoclave using a Luggin capillary. All the potentials in present work are reported versus the standard hydrogen electrode (SHE) referred to in the work of Yang [17], if not otherwise mentioned.

2.3. Materials and preparation methods

TC11 titanium alloy with a nominal composition (in wt.%) of Al 6.5%, Mo 3.5%, Zr 1.5%, Si 0.3%, and Ti as balance was used in this study. The sodium sulfate was analytical grade pure, and solutions were prepared with deionized water. Surface preparation of TC11 alloy consists of grinding the sample up to 3000-grit silicon carbide paper, degreased ultrasonically with ethyl alcohol, rinsed with distilled water and then drying in air. The electrochemical experiments were carried out in naturally aerated solutions, and the initial oxygen concentrations were approximately 3.0 to 3.5 mg L^{-1}.

3. RESULTS AND DISCUSSION

3.1. OCP measurements

3.1.1. Effect of sodium sulfate concentration

The evolution of OCP as influenced by Na_2SO_4 concentration was studied and referred relative to standard hydrogen electrode (SHE). The changes of OCP with exposure time (Fig. 1) were measured for 2 hours after immersing the samples in naturally aerated Na_2SO_4 solution (0.005, 0.01, 0.02, 0.04, and 0.10 M) at 300 °C and 10 MPa and are typical of passive metals immersed in aerated solutions.

It was observed that the OCP at various concentrations of Na_2SO_4 solution improved markedly. This abrupt positive potential change suggests the corrosion resistance of the titanium alloy electrode. In the process of immersion, the OCP curves including two different parts. In the first part, the OCP improved rapidly due to the formation of an oxide film and further thickening of passive layer arising from the reaction between the solution and the electrode [18].

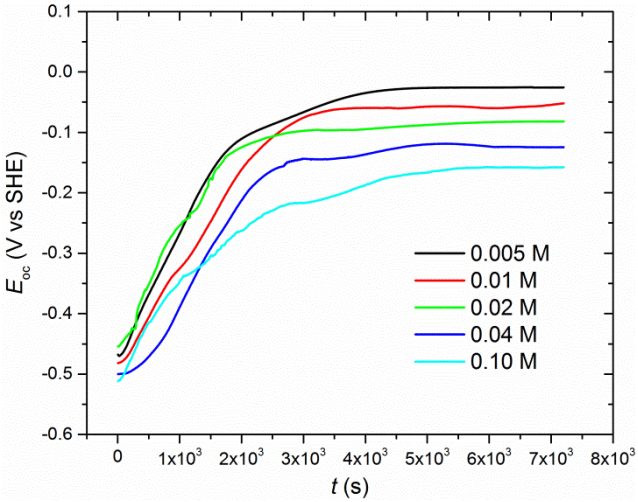

Figure 1. Curves of the change of the open-circuit potential (E_{oc}) with time obtained for the TC11 alloy in Na_2SO_4 solution of different concentrations at 300 °C, 15 MPa.

It was found that the increase keeps a logarithmic relationship with time at approximately one hour. El-Basiouny and Mazhar [19] observed that pure titanium displays similar relationship in 0.5 M Na_2SO_4 solutions for over 3 hours. They attributed it to the development of passive oxide film. In the other part, the OCP values reached a stable value with a slight shift due to the passive film attained a thickness that was steady in the solution [20].

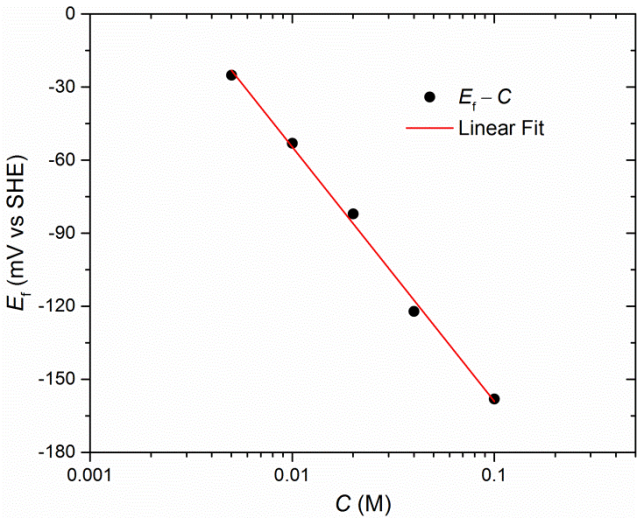

Figure 2. The relationship between the final potential (E_f) and the concentration of Na_2SO_4 solution.

Additionally, as shown in Fig. 1, the final potential value (E_f) decreased steeply with the increase of Na_2SO_4 concentration. Fig. 2 illustrates the relationship between E_f and the concentration of sodium sulfate solution, which can be given by the following equation:

$$E_f = A - B \times \log C \quad (1)$$

In Eq. (1), *A* and *B* are fitted constants. Fig. 2 shows that as the concentration of Na_2SO_4 increased from 0.005 M to 0.10 M, E_f accordingly decreased from −25 mV to −158 mV vs SHE. This may be due to more SO_4^{2-} ions adsorbed on the electrode surface of titanium alloy with the increase of Na_2SO_4 concentration [21], which would greatly reduce the OCP because of the deterioration of protection capacity of passive film. It signifies that the passive film has aggravated as the increasing Na_2SO_4 concentration. Moreover, improving the concentration of the solution, in other words, increasing the conductivity of electrolyte, and accelerating corrosion, finally resulting in decrement of the OCP.

3.1.2. Effect of temperature

Temperature can influence the kinetics and thermodynamics of a chemical reaction. It is certainly a significant electrochemical factor. Considering a typical industrial high temperature water environment, four different temperatures, 200, 250, 300, and 350 °C, were selected to study the influence of temperature on the corrosion of TC11 alloy in 0.01 M Na_2SO_4 solution at a pressure of 15 MPa.

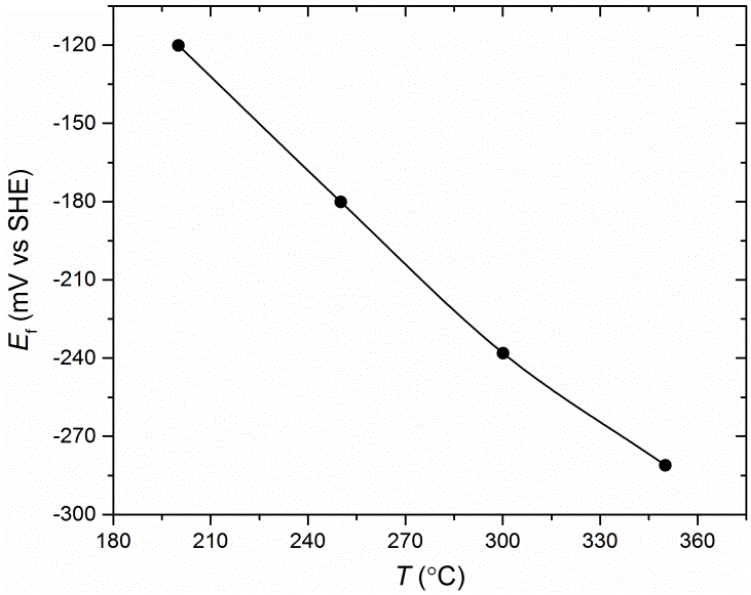

Figure 3. The variation of the final potential (E_f) as a function of temperature for the TC11 alloy in 0.01 M Na_2SO_4 solution at 15 MPa.

The OCP of the TC11 alloy electrodes was tested in 0.01 M Na_2SO_4 solution at different temperatures (200 to 350 °C) and referred to the SHE. As shown in Fig. 3, the results reveal that E_f tends to decrease with the increase of temperature, suggesting that the development of the passive film is impeded [9]. This indicates that increasing the solution temperature in favor of the deterioration of the passive film [22].

3.1.3. Effect of pressure

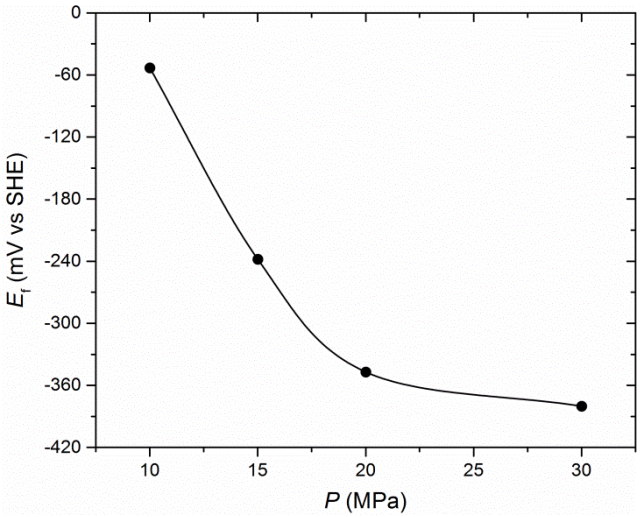

Figure 4. The variation of the final potential (E_f) as a function of pressure for the TC11 alloy in 0.01 M Na_2SO_4 solution at 300 °C.

The effect of pressure between 10 and 30 MPa on the corrosion behavior of the TC11 alloy in 0.01 M Na_2SO_4 solution at 300 °C was investigated. Fig. 4 shows the relationship between the resulting E_f values and pressure. As shown in Fig. 4, E_f tends to decrease with increasing pressure, i.e., higher pressure deteriorates the passive film, and decreases the corrosion-resistant of the alloy.

3.2. EIS measurements

EIS is a significant technique utilized to study the corrosion behavior of metal materials in harsh environment [23–27]. In present research, the EIS method was used to clarify the effect of temperature, pressure, and sulfate ion on electrochemical corrosion behavior in the TC11 alloy at high pressure hydrothermal environment.

3.2.1. Effect of Na_2SO_4 concentration

To demonstrate the influence of concentration on the corrosion of titanium alloy, the EIS tests were performed after 2 hours immersion in different concentrations of Na_2SO_4 solution at 300 °C and 10 MPa. Fig. 5 shows (a) typical Nyquist, (b) Bode phase angle, and (c) Bode $|Z|$ plots obtained for the titanium alloy after 2 hours immersion at 300 °C in Na_2SO_4 solutions of 0.005, 0.01, 0.02, 0.04, and 0.10 M. For the sake of comparison, a Nyquist plot of 0 M solution was presented in Fig. 5. As shown in Fig. 5(a), the titanium alloy electrode presented one compressed semicircle whose diameter diminish with increasing Na_2SO_4 concentration from 0.005 to 0.10 M after 2 hours immersion. Additionally, the solution exclusive of sulfate showed a bigger diameter than the sulfate solutions. The better corrosion resistance is reflected by a bigger diameter of the circle [23–26], which implies that increasing concentration in favor of the corrosion of TC11 in Na_2SO_4 solutions. It was also found that rising

concentration will increase the maximum value of the phase angle, as shown in Figure 5 (b). With the increase of concentration the phase angle curves shift toward high frequencies, but the impedance values of |*Z*| decrease at high frequencies. Moreover, |*Z*| tends to remain constant at high frequency region, whereas the values of phase angle fall to zero as the frequency increases.

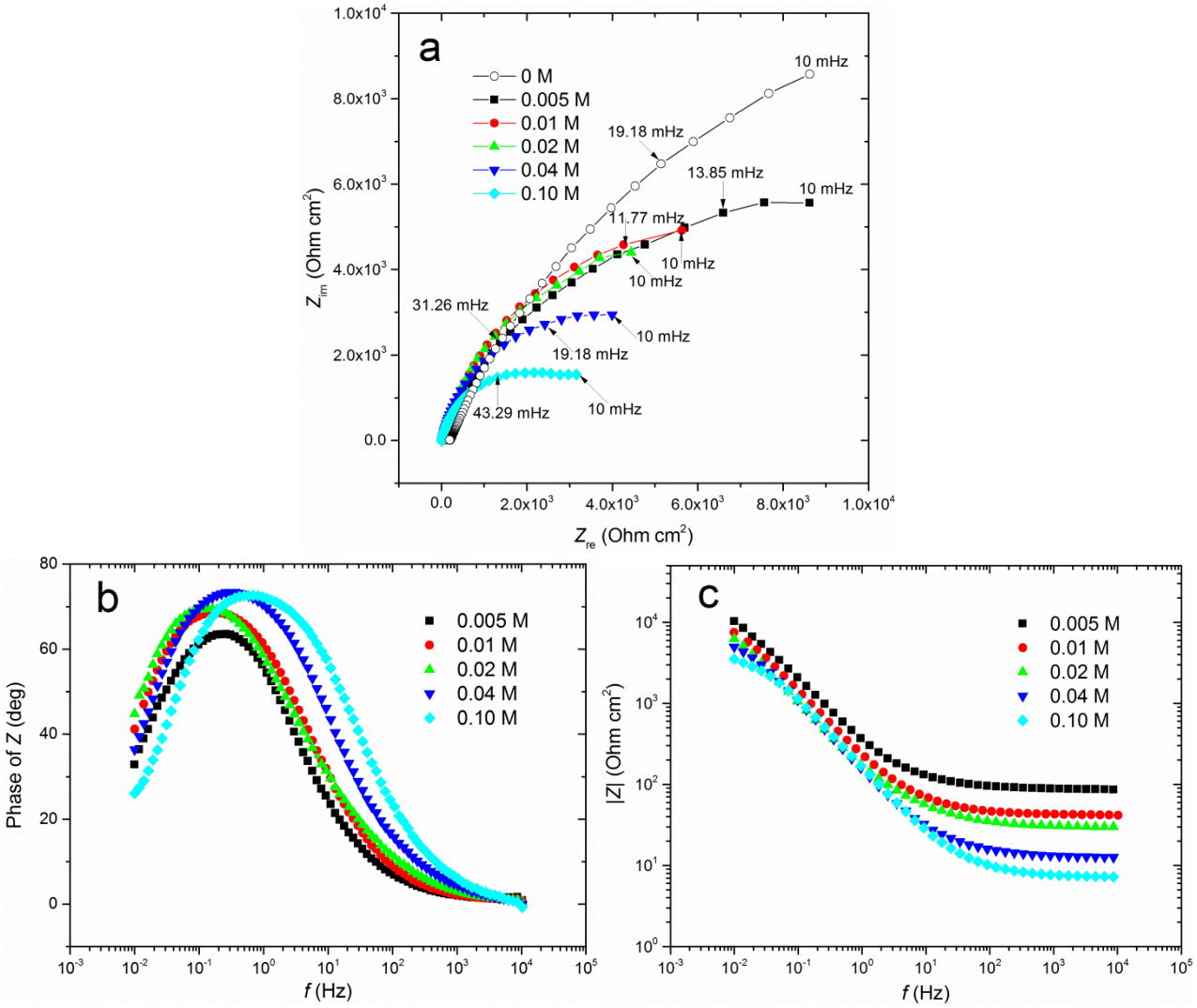

Figure 5. (a) Typical Nyquist, (b) Bode phase angle and (c) Bode |*Z*| plots obtained for the TC11 alloy after 2 h immersion at 300 °C Na_2SO_4 solution of different concentrations.

Impedance spectra involved passive films can usually be depicted by electrochemical equivalent circuits, EECs [28]. The EEC model exhibited in Fig. 6 was selected to fit the spectra shown in Fig. 5. González [29], He [30], and Liu [31] used this model to illustrate the corrosion behavior of titanium and its alloy; they explained this equivalent circuit model in theory. The proposed model in Fig. 6 is a suitable fit with the minimum of circuit elements. In each case, theories are consistent with experiments over the entire frequency range. The fitting quality was evaluated by the lower chi-square (χ^2), which were on the order of 10^{-4} to 10^{-3} [32], suggesting that the data fitted reasonably to the selected circuit. Therefore, this EEC model is reasonable to explain the corrosion mechanism of TC11 alloy in this study. This model assumes that the passive layer was not quite

compact and homogeneous [33]. The fitting results of EIS parameters are represented in Table 1. The parameters of the EEC model are defined as below: R_s is the solution resistance, Q_f represents the oxide film capacitance, R_f represents the resistance of the oxide film formed on the titanium alloy surface, Q_{dl} is the double layer capacitance, and R_{ct} represents the charge transfer resistance. The constant phase element (symbolized here by Q) is used to displace the ideal capacitance and to represent the non-ideal behavior of the capacitive components because of the heterogeneous surface that attributes to surface roughness, impurities, dislocations or grain boundaries [34].

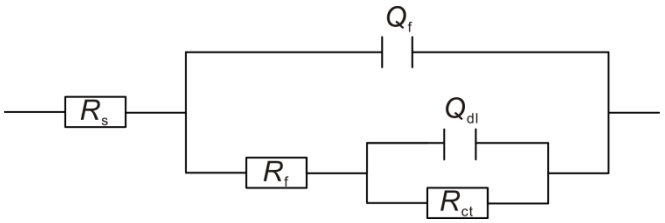

Figure 6. The equivalent circuit model used to fit the experimental data obtained by EIS measurements; the symbols of the equivalent circuit are defined in the text and their values are listed in Table 1.

Table 1. Parameters obtained by fitting the EIS data presented in Fig. 5 with the equivalent circuit shown in Fig. 6 for the titanium alloy in Na_2SO_4 solutions of different concentrations.

C (Na_2SO_4)	R_s	Q_f		R_f	Q_{dl}		R_{ct}	χ^2 ($\times 10^3$)
M	Ω cm^2	Y_0/S s^n cm^{-2}	n	Ω cm^2	Y_0/S s^n cm^{-2}	n	Ω cm^2	
0.005	38.28	0.001241	0.7925	156.90	0.0003527	0.9661	5780	1.76
0.01	18.31	0.001582	0.8234	46.89	0.0008950	0.8770	5605	0.485
0.02	13.19	0.001621	0.8177	32.46	0.001596	0.8894	5107	1.02
0.04	5.54	0.001725	0.8492	9.98	0.001401	0.8866	3179	0.405
0.10	3.16	0.001577	0.8711	6.33	0.001312	0.8696	1783	0.449

Table 1 shows that the increase of solution concentration from 0.005 M to 0.10 M decreased the values of resistances R_s, R_f, and R_{ct}. The decrease of R_s was due to the increased conductivity of the solution with the increase of solution concentration. There is no doubt that an increased concentration of solution will increase the electrical conductivity of the solution. For materials in high temperature water, the slower oxygen diffusion process across the oxide films leads to lower corrosion resistance [35, 36]. The impedance modulus $|Z|$ at low frequency is supposed to reflect how difficult oxygen diffuses through the oxide layer into the substrate [37]. It was seen from Fig. 6(c) that as increasing concentration the impedance modulus $|Z|$ at low frequency tends to decrease due to the less protective oxide films. This is consistent with the decreased R_f shown in Table 1. Moreover, the increase of concentration increases the degree of degradation of oxide film (that prevent or separate it from being further deteriorated by the aggressive SO_4^{2-} ion) formed on the surface of the titanium alloy, therefore, accelerates its dissolution in the aggressive Na_2SO_4 solution. The parameters exhibited in Table 1 further confirmed that. The constant phase element, Q_f, with its n value was 0.7925 for 0.005 M and shifted to 0.8711 for 0.10 M, which means that the constant phase element here represents passive film

capacitances with pores, these pores were to cover the charged titanium alloy surfaces in the aggressive Na_2SO_4 solution [38]. For the passive film, increasing the concentration decreased R_f and increased Q_f, Y_0. The high capacitance and low resistance of the films imply the comparatively low integrity of the passive film. On the other hand, for the TC11 alloy electrode double layer, increasing the concentration resulted in a decrease in the R_{ct} values. The decreased R_{ct} values indicate that increased solution concentration leads to solution ions that can be more easily transferred in the electric double layer, which enhance the electrochemical corrosion of TC11 alloy. In the solution containing sulfate, it was found that R_f decreases as increasing the sulfate ion concentration [11]. Therefore, sulfate ion in favor of promoting the general corrosion [13] of Ti and its alloy. This confirms that the corrosion of titanium alloy in Na_2SO_4 solution increases with increasing solution concentration at high temperature.

3.2.2. Effect of temperature

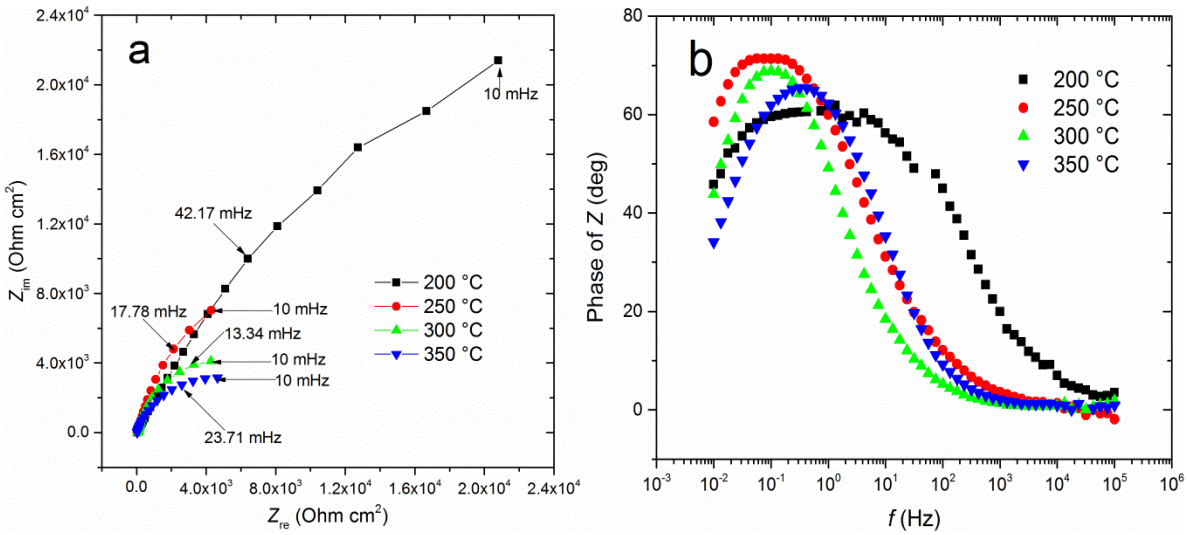

Figure 7. (a) Typical Nyquist and (b) Bode phase angle plots obtained for the TC11 alloy after 2 h immersion in 0.01 M Na_2SO_4 solution of different temperatures.

Temperature can appreciably affect the thermodynamics, interaction kinetics, and the properties of the passive film. EIS tests were performed to investigate the influence of temperature on the corrosion behavior of TC11 alloy. Nyquist and Bode plots for TC11 at different temperatures are presented in Fig. 7. Under the effect of temperature, the general shape of the impedance plots keep reserved. The same EEC exhibited in Fig. 6 was utilized to simulate the alloy/film/solution interface. The fitting results of EIS parameters are presented in Table 2. The results indicate that the R_{ct} of double-layer decreased as the temperature increased, implying that charge transfer was facilitated at the double layer. For the TC11 alloy oxide film, increasing the temperature resulted in a smaller R_f value and a larger Q_f, Y_0 value. The bigger capacitance and lower resistance of the films suggest the decreased development of the passive film. The corrosion rate of titanium and its alloy increases as the temperature increases, as observed by Bazeleva [39] and Fekry [11], and they attributed the reduced

oxide film resistance to increasing solubility of passive film. Generally, the results suggest that decreasing the solution temperature facilitates the development of a passive film, which offers excellent protection for the TC11 alloy.

Table 2. Equivalent circuit parameters of the sample after 2 h immersion in 0.01 M Na_2SO_4 solutions of different temperatures.

T °C	R_s Ω cm^2	Q_f Y_0/S s^n cm^{-2}	n	R_f Ω cm^2	Q_{dl} Y_0/S s^n cm^{-2}	n	R_{ct} Ω cm^2	χ^2 (×10^3)
200	10.44	0.0002574	0.7388	51.78	0.0002129	0.6535	42960	1.14
250	14.26	0.001431	0.7958	32.05	0.001266	0.8813	14610	0.861
300	19.07	0.001639	0.8184	27.62	0.001535	0.8996	4925	0.680
350	16.43	0.001180	0.8533	17.55	0.001043	0.7475	3702	0.113

3.2.3. Effect of pressure

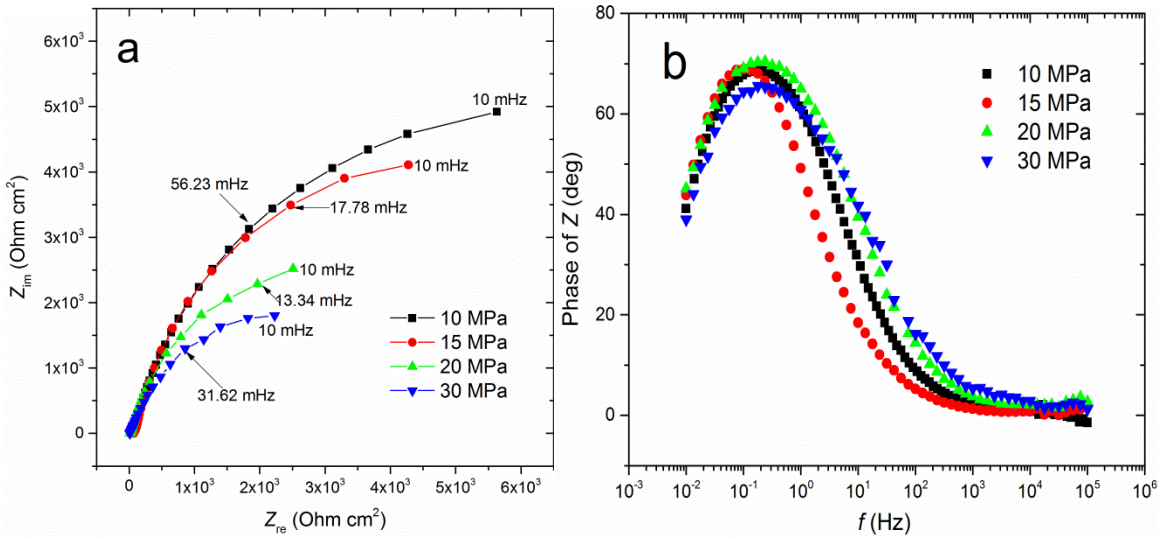

Figure 8. (a) Typical Nyquist and (b) Bode phase angle plots obtained for the TC11 alloy after 2 h immersion in 0.01 M Na_2SO_4 solution of different pressures.

To better highlight the influence mechanism of high pressure, the corrosion behavior of TC11 alloy under four pressures was studied during immersion. EIS measurements were performed on TC11 in 0.01 M Na_2SO_4 solution at 300 °C and 10, 15, 20, and 30 MPa, respectively. The Nyquist and Bode plots for TC11 at various pressures are presented in Fig. 8. Under the effect of pressure, the general shape of the impedance plots keep reserved as with the effect of concentration and temperature. The same EEC presented in Fig. 6 was utilized to simulate the alloy/film/solution interface. The fitting impedance results are shown in Table 3.

Table 3. Equivalent circuit parameters of the sample after 2 h immersion in 0.01 M Na_2SO_4 solutions of different pressures.

P MPa	R_s Ω cm^2	Q_f Y_0/S s^n cm^{-2}	n	R_f Ω cm^2	Q_{dl} Y_0/S s^n cm^{-2}	n	R_{ct} Ω cm^2	χ^2 (×10^3)
10	18.31	0.001582	0.8234	46.89	0.000895	0.8770	5605	0.485
15	19.07	0.001631	0.8184	27.62	0.001535	0.8996	4925	0.680
20	5.06	0.001579	0.8358	9.82	0.002327	0.8332	3031	0.743
30	4.49	0.001958	0.8063	7.03	0.003015	0.7648	2455	1.91

In this experiment, EIS is measured under different pressure conditions, mainly to obtain the transfer resistance R_{ct} to study the dissolution behavior and corrosion mechanism of the TC11 alloy. EIS spectra measured at different pressures consist of two parts: a non-faradaic process (corrosion product film) and a faradaic process (electrochemical reactions). Therefore, the charge transfer resistance (R_{ct}) can be used to characterize electrochemical reactions, the resistance of the corrosion products film R_f can be related to the extent of corrosion, while the inverse of the sum, $1/(R_{ct} + R_f)$, can be used to express the corrosion rate to some extent. The variations of the above parameters versus to pressure are depicted in Fig. 9. It is shown that, as pressure increases, the R_{ct} value was reduced from 5603 Ω cm^2 at 10 MPa to 2455 Ω cm^2 at 30 MPa, which implies that the electrochemical reactions are accelerated at higher pressure. R_{ct} values directly reflect the corrosion-resistant of the passive film, so with the increase of pressure, the corrosion-resistant of the titanium alloy degrades. The variations of R_f reveal an apparent decrease in R_f with increasing pressure. This is consistent with the R_{ct} results, indicating that the alloy shows a lower corrosion resistance at higher pressure. The variations of R_{ct} of the titanium alloy electrode and R_f of the passive film indicate that pressure has a significant effect on the compactness and structure of passive film. Zhang [16] claimed high pressure resulted in the inhomogeneity of the passive film as well as diminished the quantity of anti-corrosion oxides in the film. Furthermore, pressure can decrease the intensity of the passivation layer, which further decreases the corrosion-resistant.

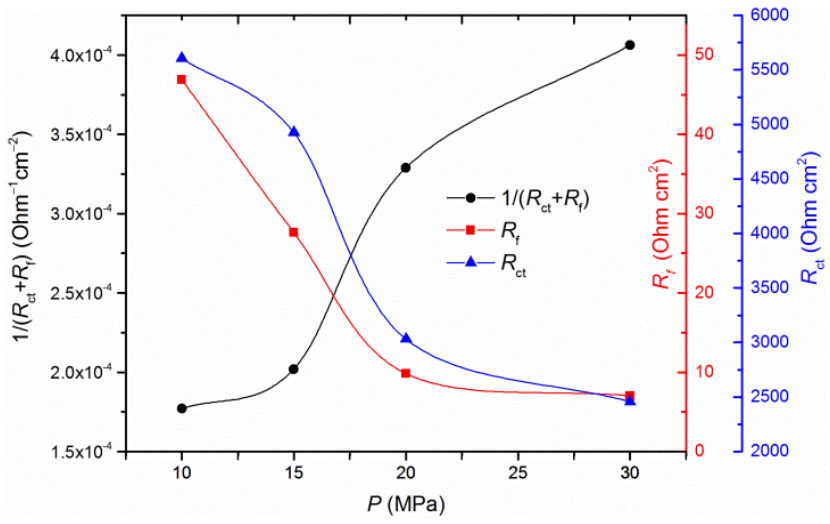

Figure 9. The variation of R_{ct}, R_f, $1/(R_{ct} + R_f)$ as a function of pressure.

3.3. Potentiodynamic polarization (PDP) measurements

3.3.1. Effect of Na_2SO_4 concentration

The PDP technique is often used to investigate the corrosion behavior of metal materials in aggressive conditions. With the purpose of understanding the influence of concentration on the corrosion behavior of the TC11 alloy, PDP curves were obtained after 2 hours of immersion in 0.005, 0.01, 0.02, 0.04, and 0.10 M Na_2SO_4 solution at 300 ℃ as shown in Fig. 10.

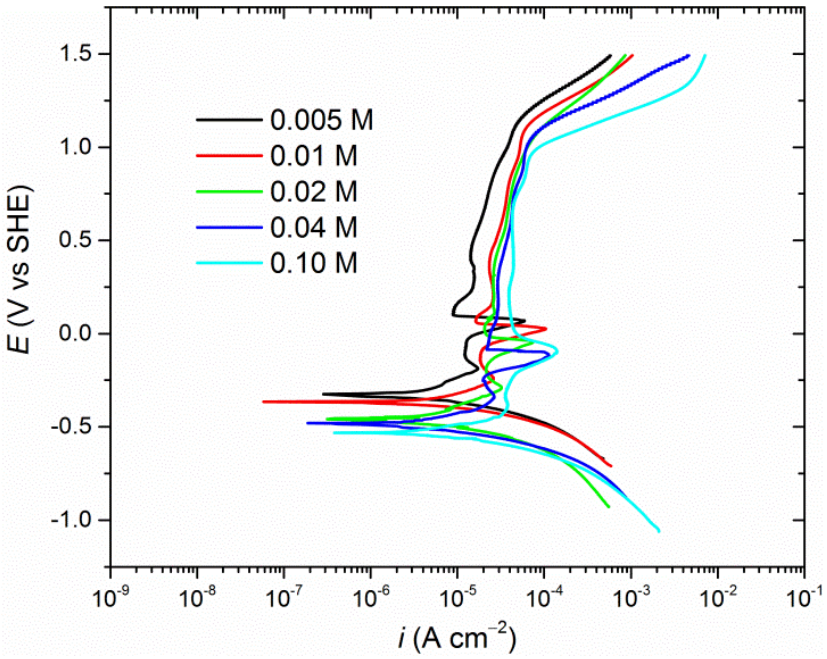

Figure 10. PDP curves obtained for titanium alloy electrode in 0.005, 0.01, 0.02, 0.04, and 0.10 M Na_2SO_4 solutions at 300 °C and 10 MPa, with a scan rate of 1 mV s^{-1}.

For all tested electrodes, the values of the corrosion parameters, corrosion potential (E_{corr}), corrosion current density (i_{corr}), Tafel slopes (β_a and β_c), passive current density (i_{pp}), and corrosion rate (R_{corr}) were calculated and presented in Table 4 as a function of Na_2SO_4 concentration. The values of i_{corr} and E_{corr} were acquired from the extrapolation of anodic and cathodic Tafel lines lay near the linear current regions. The Tafel constants were calculated as the slope of the points 50 mV after E_{corr} to ensure the presence of linearity in the Tafel slope region of the obtained polarization curves. Additionally, the values of R_{corr} (millimeter per year, mm y^{-1}) were calculated using equation [40]:

$$R_{corr} = i_{corr}\, k\, E_W/d \qquad (2)$$

where k accounts for a constant (k = 3.272 × 10^{-3} mm g μA^{-1} cm^{-1} a^{-1}), E_W represents the equivalent weight of titanium alloy (E_W calculated = 12.01), d is the density in g cm^{-3} (d = 4.5), and i_{corr} is the corrosion current density in μA cm^{-2}.

Table 4. Corrosion parameters obtained from the potentiodynamic polarization measurements for the titanium alloy electrode that was immersed in Na_2SO_4 solutions of different concentrations.

C (Na_2SO_4) M	E_{corr} mV	i_{corr} μA cm^{-2}	β_a mV dec^{-1}	β_c mV dec^{-1}	i_{pp} μA cm^{-2}	E_{tp} mV	R_{corr} mmy^{-1}
0.005	–327.6	1.13	65.8	–36.4	18	1192	9.87×10^{-3}
0.01	–366.3	3.52	87.7	–65.2	27	1142	3.07×10^{-2}
0.02	–459.6	4.56	186.5	–110.2	34	1092	3.98×10^{-2}
0.04	–485.5	6.87	394.6	–115.2	40	1062	6.00×10^{-2}
0.10	–530.6	10.45	397.7	–123.7	52	982	9.13×10^{-2}

The five polarization curves present a similar trend, which indicates the same corrosion mechanism in different concentration Na_2SO_4 solutions. In all cases, the anodic curves for the alloy show an extremely steep active dissolution region following a small active-passive peak and ending in a current independent platform. The active-passive peak attributes to metal oxidation, and a second active-passive peak followed by a steady and large passivation region of potential is invariably obtained for the alloy. The longer passive domain (from 0.13 V to 1.20 V for the 0.005 M curve) is a consequence of forming a passive film that primarily contains TiO_2 [41] and blocks the current flow. Moreover, the second passive region measured is higher than the first one, indicating good corrosion-resistant of passive films formed in this region.

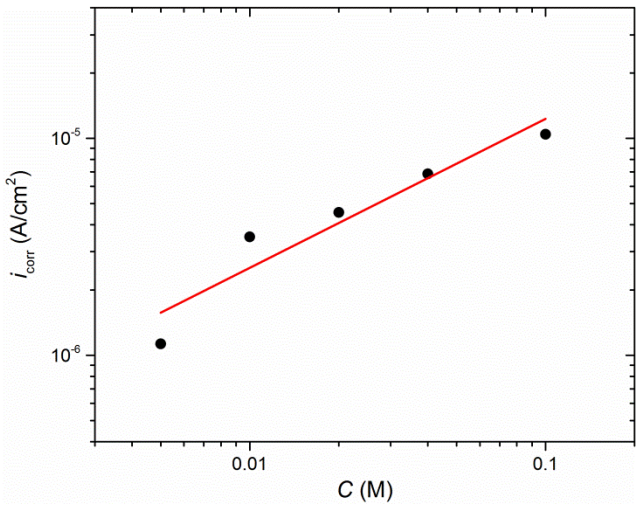

Figure 11. The variation of the logarithm of the corrosion current density (i_{corr}) with the logarithm of the concentration of Na_2SO_4 solution at 300 °C.

This passive region may be because of forming an oxide of low valence, Ti_2O_3 [42], but being an unsteady species in solution, it is swiftly oxidized to TiO_2 [43]. Eventually, a transpassive region is exhibited, as the applied potential increases the corrosion current density rises rapidly. The transpassive performance shown by the titanium alloy over 1.20 V in aerated solution is attributed to

the oxidation of TiO_2 to Ti_2O_5 [44]. Nevertheless, there is always the possibility of formation of other titanium compounds such as $TiOSO_4$ if the solution contains other species [45].

However, at all concentrations, the cathodic polarization curves are similar in nature for the TC11 alloy. This means that the same cathodic reaction takes place on the surface of the TC11 alloy. The absolute value of cathodic Tafel slopes was between 36 and 124 mV dec^{-1} in the present case. The values are approximate to the value of the hydrogen evolution reaction occurs at Ti in acidic solution [46].

The results listed in Table 4 mean that the increase of the solution concentration shifted the E_{corr} and transpassive potential (E_{tp}) toward negative values and both i_{corr} and i_{pp} increased. The corrosion potentials obtained from the OCP tests are extremely higher than those determined from the PDP measurements. The passive film on the surface was at least partially removed because the PDP tests were began with a highly reducing initial cathodic potential relative to the OCP. It is observed that increasing the concentration has a remarkably effected on the i_{corr} and as a consequence on the corrosion rate. This performance is clarified in Fig. 11 for the alloy. As the result indicates, the relationship between log i_{corr} and log C is linear for the tested alloy in accordance with the following equation [11, 47]:

$$\log i_{corr} = a + n \log C \quad (3)$$

where i_{corr} indicates the corrosion rate, C represents the molar concentration of Na_2SO_4, a and n are two empirical constants (a accounts for the value of log i_{corr} at C =1 M and the slope of the fitting line, n, is considered as the electrochemical reaction order [48]). From Fig. 11, the value of n for the TC11 alloy is approximately 0.6. Additionally, the positive slope for the alloy means that there is a positive correlation between the corrosion rate and Na_2SO_4 concentration, where the i_{corr} value rises as the aggressiveness of the solution increases.

Passive current density (i_{pp}) is usually used to evaluate the quality of the passive film formed on the surface. This is due to the normal proportional relationship between the corrosion rate of passive film and the passivation current density [49]. In all concentrations, a similar trend for passivation current density is shown. The values of passive current density slowly increase linearly with the applied potential. It indicates that increasing the potential lead to increasing metallic cations, which can facilitate the formation of the passive film or can dissolve into the solution. Because of the relative large passive current region in the potentiodynamic polarization curve, the passive current density cannot be determined at a potential below the transpassive potential. Correspondingly, the average of the passive current density was acquired by calculating the arithmetic mean between the secondary passive potential and the transpassive potential. The values of the passive current density changed from 18 μA cm^{-2} in 0.005 M Na_2SO_4 solution to more positive values of 52 μA cm^{-2} in 0.10 M Na_2SO_4 solution. This indicates that the SO_4^{2-} ion reduced the protective property of the passivation film, that is to say, promoted the dissolution of the passivation film. This is consistent with the increased i_{corr}.

Therefore, the PDP results are consistent with the data acquired from the EIS tests. This indicates that the corrosion of titanium alloy increases in a higher concentration of Na_2SO_4 solution.

3.3.2. Effect of temperature

The effect of temperature on the electrochemical corrosion behavior of the TC11 alloy was investigated in 0.01 M Na_2SO_4 as illustrated in Fig. 12 and the corrosion parameters were evaluated and listed in Table 5. Firstly, the dissolution of the passive film was enhanced by increasing temperature in high temperature solution, which was proved by the increasing i_{corr} of the alloy. The results distinctly show that these parameters are affected by the temperature of the solution. The values of i_{corr} increase with temperature, indicating that the protective properties of the surface oxide film decrease resulting from its dissolution. This phenomenon is possibly ascribed to the intrinsic alterations of the film in its chemical composition and/or physical structure [50].

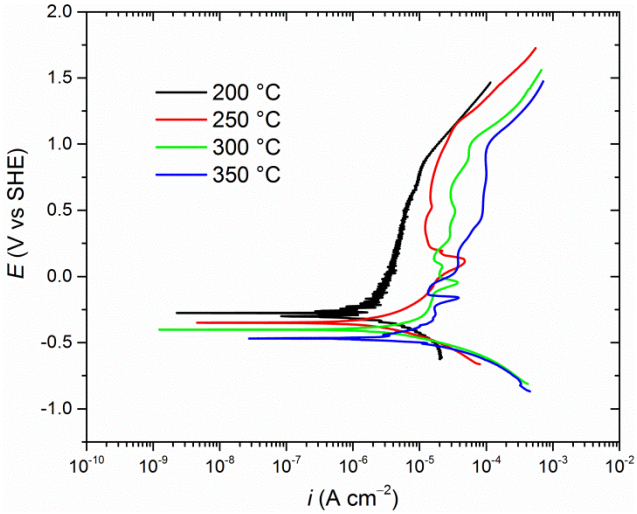

Figure 12. Potentiodynamic polarization curves obtained for titanium alloy electrode in 0.01 M Na_2SO_4 solution at 10 MPa of different temperatures, with a scan rate of 1 mV s^{-1}.

Table 5. Electrochemical parameters of the TC11 electrodes after 2 h immersion in 0.01 M Na_2SO_4 solution at different temperatures and 15 MPa

T °C	E_{corr} mV	i_{corr} μA cm^{-2}	β_a mV dec^{-1}	β_c mV dec^{-1}
200	–291.6	1.03	386.9	–87.1
250	–349.3	1.46	174.6	–104.6
300	–400.6	3.89	221.6	–105.4
350	–461.5	5.21	269.3	–117.1

Moreover, E_{corr} tends to more negative values, indicating the dissolution of the passive film. The corrosion potential is a thermodynamic concept. It is a measure of the corrosion reaction trend. A more negative corrosion potential indicates that the specimen is more prone to severe corrosion. The higher temperature helps both anodic and cathodic reactions to overcome the activation energy by providing additional energy, causing the corrosion potential to decrease and the corrosion reaction rate

to increase. This behavior occurs because increasing temperature results in a conversion of internal energy into electrochemical energy, decreasing both the anodic and cathodic polarization resistances.

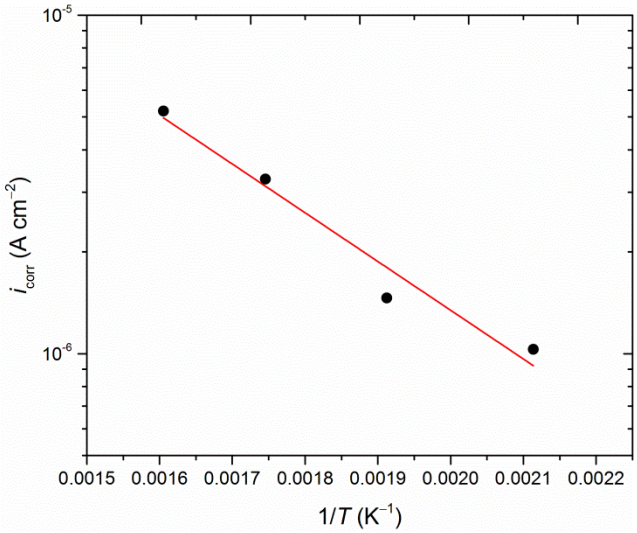

Figure 13. The variation of the logarithm of i_{corr} with $1/T$ in 0.01 M Na_2SO_4 solution.

An Arrhenius diagram of the log i_{corr} versus the $1/T$ is illustrated in Fig. 13 for the TC11 electrodes. As the result indicates, the plot is linear, and the apparent activation energy (E_a) of the corrosion process was obtained from the slope of the plot following the Arrhenius equation:

$$\log i_{corr} = A - E_a/(2.303RT) \quad (4)$$

where A is a constant, and the obtained E_a value is 27.5 kJ mol^{-1}, which is related to the susceptibility to the corrosion dissolution effect. Castle [51] proposed that the corrosion rate was restricted by the liquid state diffusion of metallic ions through pores in the oxide film. However, Robertson [52] recognized that the corrosion process was restricted by the solid phase transport of metallic ions along grain boundaries of the oxide layer. The main difference of their approaches is in the activation energy of corrosion due to different diffusion methods of metallic ions. Castle's activation energy (15–20 kJ mol^{-1}) is much lower than Robertson's (approximately 120 kJ mol^{-1}). The activation energy for solution phase diffusion is usually lower than 41.84 kJ mol^{-1} [51, 53]. For instance, Bazan [53] gave a value of 17.15 kJ mol^{-1} for the transport of ferro- and ferricyanide ions in aqueous solutions of sodium hydroxide. In this research, the relevant activation energy is 27.5 kJ mol^{-1}, which is consistent with the activation energy (lower than 41.84 kJ mol^{-1}) for liquid phase diffusion. The present activation energy is so low that the diffusion of metallic ions through pores in oxide film is primarily supposed the limiting step of the corrosion process. Therefore, the corrosion process of TC11 in 0.01 M Na_2SO_4 solution is controlled by ion diffusion in the liquid phase.

3.3.3. Effect of pressure

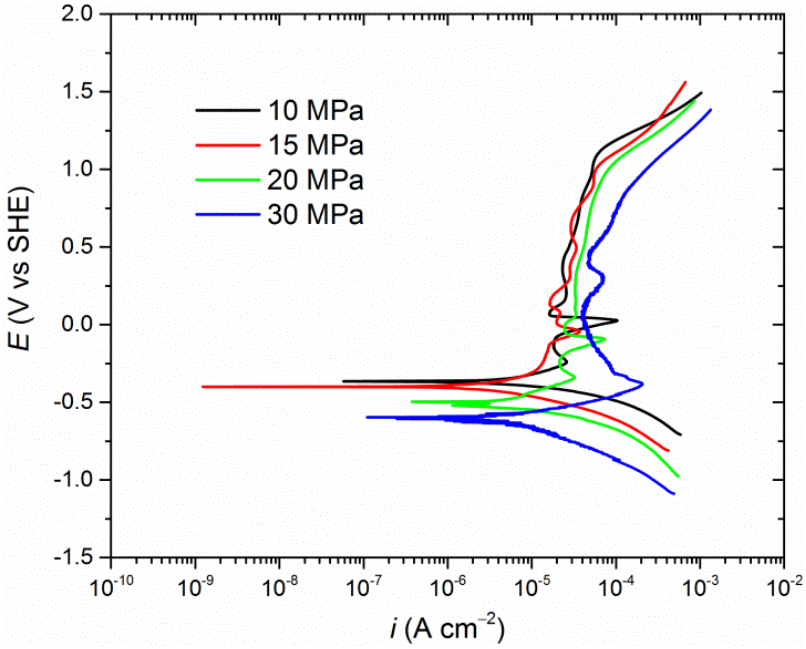

Figure 14. Potentiodynamic polarization curves obtained for titanium alloy electrode in 0.01 M Na_2SO_4 solution at 300 °C of different pressures, with a scan rate of 1 mV s^{-1}.

Potentiodynamic scans were carried out on TC11 alloy in 0.01 M Na_2SO_4 solution at a temperature of 300 °C at different pressures (10–30 MPa), and the polarization curves are presented in Fig. 14. The evaluated parameters were listed in Table 6. As the pressure increase, the corrosion potential for the alloy shifts to lower values, suggesting accelerate the anodic dissolution of the passive film. In higher pressure, SO_4^{2-} may corrode the alloy surface and can improve the formation of soluble corrosion products. This results in raising the corrosion rate (i_{corr}) for the alloy and reducing the corrosion resistance against local corrosion [54]. The decrease in E_{corr} and i_{corr} indicates that the TC11 alloy is more active under higher pressure. The alloy gains more strain energy when the pressure is increased, and the strain energy converts into electrochemical energy, making the electrochemical reaction occur more easily [55].

Table 6. Electrochemical parameters of the TC11 electrodes after 2 h immersion in 0.01 M Na_2SO_4 solution at different pressures and 300 °C.

P °C	E_{corr} mV	i_{corr} μA cm^{-2}	β_a mV dec^{-1}	β_c mV dec^{-1}
10	–366.3	3.52	87.8	–65.2
15	–400.3	3.89	221.6	–105.4
20	–496.9	4.76	178.9	–115.7
30	–613.5	6.21	132.7	–180.4

4. CONCLUSIONS

The influence of solution concentration, temperature, and pressure on the electrochemical corrosion of TC11 alloy in high temperature Na_2SO_4 solution was investigated. The study was performed by using in situ electrochemical techniques, i.e., OCP, EIS, and PDP measurements. PDP results revealed that the increase of either concentration or temperature and pressure shifted the values of E_{corr} for the alloy toward the negative direction, and increased the values of i_{corr} and R_{corr}. The oxide film resistance (R_f) value and charge transfer resistance (R_{ct}) confirmed these results.

The effect of the temperature gave rise to the determination of the activation energy of the corrosion process. The corrosion process was limited by the liquid phase transport of metallic ions through pores in the oxide film.

Higher temperatures and pressures make the electrochemical corrosion reaction occur more easily, and accelerate the deterioration of passive film.

ACKNOWLEDGEMENTS
This work was financially supported by the National Key Research and Development Plan (2016YFC0600100), 135 Program of the Institute of Geochemistry, Chinese Academy of Sciences (CAS), and Large-scale Scientific Apparatus Development Program (YZ200720), CAS.

References

1. R. Narayanan and S.K. Seshadri, *Corros. Sci.*, 50 (2008) 1521.
2. J. Vaughan and A. Alfantazi, *J. Electrochem. Soc.*, 153 (2006) B6.
3. Y. Kurata and M. Son, *Rev. High Pressure Sci. Technol.*, 11 (2001) 324.
4. J-J. Park, S-I. Pyun and S-B. Lee, *Electrochim. Acta*, 49 (2004) 281.
5. J-M. Le Canut, S. Maximovitch and F. Dalard, *J. Nucl. Mater.*, 334 (2004) 13.
6. Y.Z. Chen, M. Urquidi-Macdonald and D.D. Macdonald, *J. Nucl. Mater.*, 348 (2006) 133.
7. D-J. Kim, H-C. Kwon and H.P. Kim, *Corros. Sci.*, 50 (2008) 1221.
8. H. Sun, X.Q. Wu and E.H. Han, *Corros. Sci.*, 51 (2009) 2565.
9. A.A. Mazhar, *J. Appl. Electrochem.*, 20 (1990) 494.
10. P. Botella, C. Frayret, T. Jaszay and M.H. Delville, *J. Supercrit. Fluid*, 25 (2003) 269.
11. A.M. Fekry, *Electrochim. Acta*, 54 (2009) 3480.
12. J. Liu, A. Alfantazi and E. Asselin, *J. Electrochem. Soc.*, 162 (2015) C189.
13. B. Deng, Y.M. Jiang, J.X. Liao, Y.W. Hao, C. Zhong and J. Li, *Appl. Surf. Sci.*, 253 (2007) 7369.
14. Y.G. Yang, T. Zhang, Y.W. Shao, G.Z. Meng and F.H. Wang, *Corros. Sci.*, 52 (2010) 2697.
15. B. Liu, T. Zhang, Y.W. Shao, G.Z. Meng, J.T. Liu and F.H. Wang, *Int. J. Electrochem. Sci.*, 7 (2012) 1864.
16. C. Zhang, Z.W. Zhang and L. Liu, *Electrochim. Acta*, 210 (2016) 401.
17. I-J. Yang, *Mater. Chem. Phys.*, 49 (1997) 50.
18. E.A.A. El Meguid and A.A.A. El Latif, *Corros. Sci.*, 49 (2007) 263.
19. M.S. El-Basiouny and A.A. Mazhar, *Corrosion*, 38 (1982) 237.
20. I.C. Lavos-Valereto, I. Costa and S. Wolynec, *J. Biomed. Mater. Res.*, 63 (2002) 664.
21. H.P. Leckie and H.H. Uhlig, *J. Electrochem. Soc.*, 113 (1966) 1262.
22. K. Galić, M. Pavić and N. Ciković, *Corros. Sci.*, 36 (1994) 785.
23. J.R. Macdonald, *Ann. Biomed. Eng.*, 20 (1992) 289.
24. B-Y. Chang and S-M. Park, *Annu. Rev. Anal. Chem.*, 3 (2010) 207.

25. E.S.M. Sherif, A.A. Almajid, A.K. Bairamov and E. Al-Zahrani, *Int. J. Electrochem. Sci.*, 7 (2012) 2796.
26. E.S.M. Sherif, *Int. J. Electrochem. Sci.*, 7 (2012) 2832.
27. L.Y .Xu, M. Li, H.Y. Jing and Y.D. Han, *Int. J. Electrochem. Sci.*, 8 (2013) 2069.
28. A.K. Shukla and R. Balasubramaniam, *Corros. Sci.*, 48 (2006) 1696.
29. J.E.G. González and J.C. Mirza-Rosca, *J. Electroanal. Chem.*, 471 (1999) 109.
30. X.H. He, J.J. Noël and D.W. Shoesmith, *J. Electrochem. Soc.*, 149 (2002) B440.
31. J. Liu, A. Alfantazi and E. Asselin, *Corrosion*, 70 (2014) 29.
32. S.L. de Assis, S. Wolynec and I. Costa, *Electrochim. Acta*, 51 (2006) 1815.
33. J.F. Zhang, W. Zhang, C.W. Yan, K.Q. Du and F.H. Wang, *Electrochim. Acta*, 55 (2009) 560.
34. F.B. Growcock and R.J. Jasinski, *J. Electrochem. Soc.*, 136 (1989) 2310.
35. R.D. Armstrong and K. Edmondson, *Electrochim. Acta*, 18 (1973) 937.
36. J. Robertson, *Corros. Sci.*, 32 (1991) 443.
37. X.H. Liu, X.Q. Wu and E.H. Han, *Electrochim. Acta*, 108 (2013) 554.
38. E.S.M. Sherif, A.T. Abbas, D. Gopi and A.M. El-Shamy, *J. Chem.* (2014) Doi: 10.1155/2014/538794.
39. N.A. Bazeleva, *Mater. Sci.*, 42 (2006) 691.
40. ASTM G 102-89: *Standard Practice for Calculation of Corrosion Rates and Related Information from Electrochemical Measurements*, 2010.
41. I. Milošev, M. Metikoš-Huković and H-H. Strehblow, *Biomaterials*, 21 (2000) 2103.
42. M. Pourbaix, *Atlas of Electrochemical Equilibria in Aqueous Solutions*, (1974), NACE, Houston.
43. C.E.B. Marino, E.M. de Oliveira, R.C. Rocha-Filho and S.R. Biaggio, *Corros. Sci.*, 43 (2001) 1465.
44. T. Eliades, *Int. J. Oral Maxillofac. Implants*, 12 (1997) 621.
45. M. Bojinov, P. Kinnunen, K. Lundgren and G. Wikmark, *J. Electrochem. Soc.*, 152 (2005) B250.
46. E.J. Kelly and H.R. Bronstein, *J. Electrochem. Soc.*, 131 (1984) 2232.
47. M.A. Ameer, A.M. Fekry and F. El-Taib Heakal, *Electrochim. Acta*, 50 (2004) 43.
48. M.A. Ameer, A.A. Ghoneim, A.M. Fekry and E.T. Heakal, *Materialwiss Werkst*, 37 (2006) 589.
49. C. Liu, A. Leyland, Q. Bi and A. Matthews, *Surf. Coat. Technol.*, 141 (2002) 164.
50. S. Ningshen, U.K. Mudali and R.K. Dayal, *Brit. Corros. J.*, 36 (2001) 36.
51. J.E. Castle and H.G. Masterson, *Corros. Sci.*, 6 (1966) 93.
52. J. Robertson, *Corros. Sci.*, 29 (1989) 1275.
53. J.C. Bazan and A.J. Arvia, *Eletrochim. Acta*, 10 (1965) 1025.
54. V. Branzoi, F. Golgovici and F. Branzoi, *Mater. Chem. Phys.*, 78 (2002) 122.
55. Q.Y. Liu and H.P. Li, *Miner. Eng.*, 23 (2010) 691.